RSC Advances

COMMUNICATION

View Article Online
View Journal | View Issue

Cite this: *RSC Adv.*, 2015, **5**, 94855

Received 31st August 2015
Accepted 24th October 2015

DOI: 10.1039/c5ra17622k

www.rsc.org/advances

Starch–borate–graphene oxide nanocomposites as highly efficient targeted antitumor drugs†

Rumei Cheng,[a] Shengju Ou,[b] Yexu Bu,[a] Xuan Li,[a] Xiaohong Liu,[a] Yuqin Wang,[a] Rui Guo,[a] Bingyang Shi,[c] Dayong Jin*[cd] and Yong Liu*[ac]

We synthesized novel borate antitumor drugs sourced from starch–borate–graphene oxide (SBG) nanocomposites. *In vitro* results suggest that SBG from the molar ratio of $n_{starch} : n_{borate} : n_{GO}$ at 2 : 1 : 1 exhibits excellent biocompatibility with normal human cells (>90% cell viability), but are highly toxic against cancer cells (<20% cell viability).

Boron (B), the fifth element in the periodic table, is widely found in nature in the form of borate compounds, and has been known for some time as an essential micronutrient in the growth and viability of plants. Boric acid and other related boron containing compounds have been found to influence some biological processes in the presence of proteins, polysaccharides and glycoproteins.[1,2] Research by the U.S. Department of Agriculture and other researchers has indicated that boron is nutritionally important in animal and human homeostasis.[3] A reference dose of 0.3 mg B per kg per day and an acceptable daily intake of 16.5 mg B per day are estimated as a nutritional requirement.[4] The other studies, however, showed that the borate exhibited developmental toxicity and reproductive toxicity in some mammalian species.[5,6] Therefore various biocompatible molecules such as polyols have been incorporated to improve the biocompatibility of borates. Complexation of borate anions with polysaccharides and polyols in aqueous solutions were prepared elsewhere as hydrogels and films and were found useful as drug delivery carriers.[7] A glucose-triggered drug delivery system was also achieved *via* crosslinkage between the borate and poly(vinyl alcohol).[8] Further work regarding the borate–chitosan complex as antimicrobial and antifungal drugs was reported recently.[9] These investigations have greatly expanded the understanding of the biological and pharmaceutical applications of boron-containing compounds. Particularly, antitumor activity of boron compounds has been recognized in some reports. Presence of the empty p-orbital of boron provides active sites for biological nucleophiles of enzyme residues (such as serine) and hydroxyl groups from carbohydrates and nucleic acids, leading to inhibition of serine and several proteases.[10,11] For example, a dipeptide boronic acid composite based antitumor drug called bortezomib (BTZ) has been marked as Velcade (Millenium Pharmaceuticals).[12] The inhibition ability of BTZ against cancer cell was attributed to the direct binding between boronic acid group and threonine residues in the active sites of several proteases. However, BTZ doesn't work well with many solid tumors and is suffered to dose-limiting toxicity to cancer cells over the normal cells.[13] Though catechol-polymers were conjugated with BTZ to improve selectively targeting to cancer cells, sensitive concentration of normal cells to BTZ was still very low.[14] Enhanced biocompatibility of borate compounds with normal cells while remained toxicity against cancer cells is still a big challenge for borate based antitumor drugs. Starch is an abundant, inexpensive, renewable and fully biodegradable material.[15] It contains numerous hydroxyl groups available for modification of the borate. In this work, a biocompatible starch was first used to bioconjugate the boric acid to increase its drug delivery efficacy. The as-synthesized starch–borate (SB) complex in this work exhibited good antitumor activity against human tumorous choroidal melanoma (CM) cells. The targeting delivery of the SB complex towards tumor cells and biocompatibility of the SB against normal cells, however, were quite poor. The newly attractive 2D materials graphene based derivative *e.g.* graphene oxide was thus introduced to enhance both the targeting ability against tumor cells and biocompatibility with normal ocular cells.

The new-generation carbon nanomaterials of graphene and its derivative *e.g.* graphene oxide (GO) have recently attracted ever

[a]*Institute of Advanced Materials for Nano-Bio Applications, School of Ophthalmology & Optometry, Wenzhou Medical University, Wenzhou, Zhejiang 325027, China. E-mail: yongliu1980@hotmail.com*

[b]*Nanjing Landa Femtosecond Insepection Techonlogy Co. Ltd., Nanjing High-tech Industry Development Zone, Nanjing, Jiangsu 210032, China*

[c]*ARC Center of Excellence for Nanoscale BioPhotonics, Department of Chemistry and Biomolecular Science, Macquarie University, Sydney, NSW 2109, Australia*

[d]*Institute for Biomedical Materials and Devices, Faculty of Science, University of Technology Sydney, NSW 2007, Australia. E-mail: dayong.jin@uts.edu.au*

† Electronic supplementary information (ESI) available: Experimental section, TEM, cell viability. See DOI: 10.1039/c5ra17622k

increasing interests both for its implications in fundamental science and for potential numerous applications due to their unique nanoscale structures and physicochemical properties.[16,17] Of particular interest to cross-discipline researchers is the interaction between the graphene-based nanomaterials and biomolecules in the areas of cell biology systems.[18] Numerous studies have confirmed that the graphene-based scaffolds were compatible with live cells by supporting both their growth and their adhesive properties.[19,20] The GO–doxorubicin hydrochloride hybrid was reported as the effective drug delivery system.[21] The PEGylate–GO composite exhibited efficient delivery of camptothecin to colon cancer cells.[22] Incorporation of GO with polymer based drug has been found to significantly improve the tumor passive uptake of the polymer complexes *via* enhanced permeability and retention (EPR) effects, which allows effective preferential transport of therapeutic agents to tumor sites *via* its carbon base.[23] Our previous work reported a highly pH-sensitive antitumor drug based on the GO modified chitosan-xanthone Schiff base.[24]

In this work, we incorporated a unique 2-dimensional nanosheet graphene oxide (GO) to carry the starch–borate complex for enhanced delivery and loading efficiency of the starch–borate complex. We developed a novel structure by covalently linking the oxygen-containing functional groups of GO with starch–borate, and designed the novel nanoscale antitumor drugs with strong toxicity against cancer cells and good biocompatibility with normal cells simultaneously. The concept presented here provides a facile and efficient way to combine the advantages of both the biologic effects of starch and borate and the 2D effect and strong penetrability ability of GO. The resulting SBG shows good biocompatibility to human normal retinal pigment epithelia (RPE) cells while possesses strong cytotoxicity against human CM cells. This is strongly suggestive of a new class of highly efficient targeting antitumor drugs.

Results and discussion

Nanocomposites with different constituent proportion ($n_{starch} : n_{borate} : n_{GO}$ = 1 : 1 : 1; 1 : 2 : 1; 1 : 3 : 1; 2 : 1 : 1; and 3 : 1 : 1) were prepared and marked as S1, S2, S3, S4, and S5 respectively. The schematic structure of SBG was shown in Fig. 1(a). It is well-known that GO is a non-biodegradable material and the non-chelated borate is potentially toxic. The use of starch as linker in the SBG complex is beneficial as it reduces the possible side effects of both borate and GO from direct interaction with cells. No precipitation was observed from the SBG suspension, even when placed and held for over one week, suggesting the outstanding dispersibility of SBG in the aqueous solution, as results of the excellent hydrophilicity of both starch and GO. Boric acid (or soluble starch with boric acid) was readily covalently linked to GO at the identified conditions without occurrence of any precipitation. The dried SBG were easily dispersible in very dilute aqueous solution *via* ultrasonication.

The transmission electron microscopy (TEM) image in Fig. 1(b) shows the typical flake-like shape of the resulting SBG and nearly transparent nanosheets as commonly seen in graphene based nanocomposites.[25] The thickness of the GO was

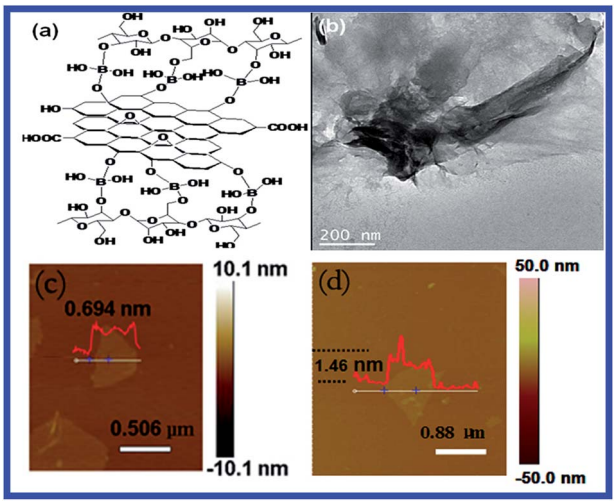

Fig. 1 (a) Schematic structure of the starch–borate–GO nanocomposite, (b) TEM micrograph of the starch–borate–GO nanocomposite, (c) AFM micrograph of GO, and (d) AFM micrograph of the starch–borate–GO nanocomposite.

determined by atomic force microscopy and found to be around 0.7 nm (Fig. 1(c)), suggesting that one layered graphene oxide sheet was prepared. The thickness of the as-synthesized SBG increased to 1.46 nm after incorporation of SB with GO (Fig. 1(d)).

To confirm the successful synthesis of SBG, a Fourier transform infrared spectroscopy (FTIR) technique was used to characterize the functionalized groups of the resulting composite. Fig. 2(a) shows that the FT-IR spectrum of GO (curve i, Fig. 2(a)) records a very simple curve with aromatic C–C stretch (in ring) at 1455 and 1340 cm^{-1}, and a weak C=O stretch at 1730 cm^{-1}. As soon as the spectrum of SBG (curve iv, Fig. 2(a)) is concerned, the peak of O–H at 3400 cm^{-1} becomes broader and stronger. A peak observed at 1646 cm^{-1} is assigned to hydroxyl group (–OH) bent vibration, indicating that starch complex was bond with GO *via* the borate mediated conjugating chemistry. The hydrogen bond interaction also existed between different molecular chains.[26] Peaks at 1060 cm^{-1}, 1379 cm^{-1}, 1724 cm^{-1} can be attributed to C–O, O–H, and C=O from carboxylic acid and carbonyl moieties, respectively. The peak at 930 cm^{-1} from the spectrum of SBG may result from the incorporation of starch with GO.[27] SBG nanocomposite was further characterised by X-ray photoelectron spectroscopy (XPS) analysis (Fig. 2(b)). The C1s peak of SBG was observed at 286.2 eV, and differed to that of GO at 285.8 eV.[28] The boron peak at 192 eV was evident in the spectrum of SBG while no such peak was observed in GO.[29] Both FT-IR and XPS confirm the presence of oxygen functional groups on the GO surface and the successful synthesis of SBG.

Structures of SBG nanocomposites were further measured by Raman spectroscopy. As shown in Fig. 2(c), two characteristic peaks at 1340 cm^{-1} (D band) and 1582 cm^{-1} (G band) due to presence of GO are identified, respectively.[30] No significant shift is observed when GO is transformed to SBG. However, the intensity ratio of D band to G band (I_D/I_G), decreased from 0.96 (for GO) to 0.88 (for SBG), suggesting improved integrity and less defects obtained by the introduction of starch into the GO.[31] We

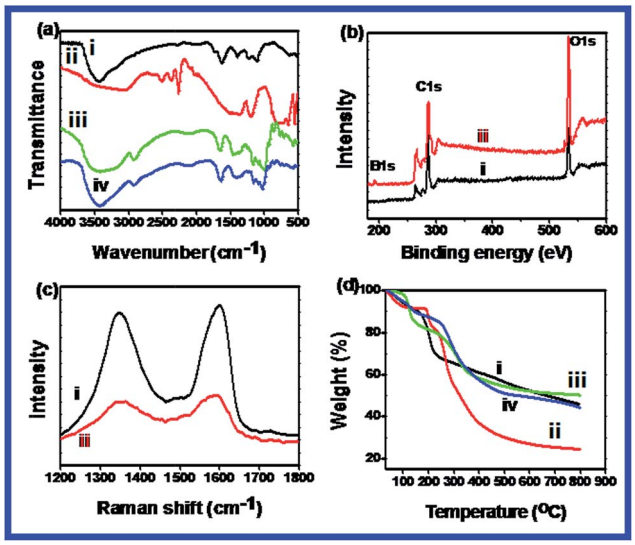

Fig. 2 (a) FT-IR spectra of various materials: (i) GO, (ii) boric acid, (iii) starch, (iv) SBG; (b) XPS survey scan spectra of (i) GO and (ii) SBG; (c) Raman spectra of (i) GO and (ii) SBG; and (d) TGA curves of (i) GO, (ii) starch, (iii) starch–borate complex, (iv) SBG.

further performed thermogravimetric analysis (TGA) on the resulting materials. TGA is a very useful technique for identifying different components of a composite.[32] As can be seen in Fig. 2(d), the weight loss for all four samples (GO, starch, starch–borate complex, and SBG) in the 50–160 °C range is attributed to the release of adsorbed water. Compared with the other three samples, SBG shows a relatively lower decomposition rate within 300 °C (curve iv, Fig. 2(d)) because of the crosslinking of borate with starch and GO.[33] However, the less thermal stability of SBG than starch–borate complex (curve iii, Fig. 2(d)) and the pristine GO (curve ii, Fig. 2(d)) is visible when the temperature is above 300 °C. This may be associated with release of borate from SBG, resulting in a fast decomposition of the isolated starch.

Cytotoxicity of SBG compared with starch–borate and GO with normal ARPE-19 cells and tumorous OCM-1 cells were evaluated using the Cell Counting Kit-8 (CCK-8) assay.[34] All samples were sterilized using anhydrous ethanol for 24 h, prior to the co-culturing with two types of cells. Concentration of each sample was remained at 50 μg mL^{-1}. The cell viability of ARPE-19 cells is shown in Fig. 3(a). Most samples (S1, S4, S5) showed the good cell viability which was higher than 70% within a 48 h culture, indicating good biocompatibility of the resulting SBG with normal cells. S4 nanocomposite ($n_{starch} : n_{borate} : n_{GO}$ = 2 : 1 : 1) exhibited much higher cell viability compared to the other samples for different incubation times. Low cytotoxicity of GO is also observed, well consistent with our previous studies.[35] The pristine borate, however, shows a slightly high cytotoxicity. It can be seen in Fig. 3(a) that cytotoxicity of the resulting SBG is dependent on the amount of borate present. The cell viability decreased from 90% to 60% in 48 h when the concentration of borate increased from 25% (S4) to 50% (S2). Sample S3 possesses the highest amount of borate and thus exhibits the lowest ARPE-19 cell viability as shown in Fig. 3(a). As expected, cell viability became enhanced with increasing amounts of

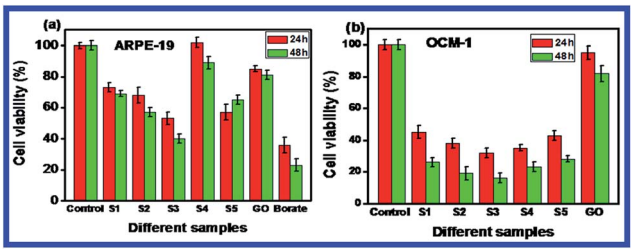

Fig. 3 Cell viability of different samples (a) with ARPE-19 cells, and (b) with OCM-1 cells. S1 to S5 are the SBG samples prepared from $n_{starch} : n_{borate} : n_{GO}$ = 1 : 1 : 1; 1 : 2 : 1; 1 : 3 : 1; 2 : 1 : 1; 3 : 1 : 1, respectively. Cell culture time: 24 h and 48 h. The concentration of all samples is 50 μg mL^{-1}. The sample without addition of nanomaterials was used as the control.

starch due to the excellent biocompatibility of starch. Particularly, the sample S5 with highest content of starch (60%) shows a slightly lower cell viability than sample S4 (50%). This is probably attributed to the relative higher percentage of GO at the sample S4 (25%) than that at the sample S5 (20%), confirming the outstanding biocompatibility properties of GO. Since borate is highly toxic to both types of human cells, it is generally not suitable as an antitumor drug which requires high toxicity against tumor cells and good biocompatibility with normal cells. Our present work demonstrates that the borate sandwiched by unique starch and graphene oxide can offer improved biocompatibility with normal cells and targeted suppressive ability against tumor cells. As shown in Fig. 3(b), OCM-1 cell viability with all samples (S1–S5) is less than 30% after 48 h incubation, suggesting good antitumor activity of the resulting SBG. Three samples (S1, S4, S5) which possess good biocompatibility with ARPE-19 cells exhibit good inhibition ability against OCM-1 cells. Of particular interest, the sample S4 shows excellent biocompatibility with ARPE-19 cells (90% cell survival rate) while remaining a superb antitumor ability with OCM-1 cells (20% cell viability), suggesting that as a promising

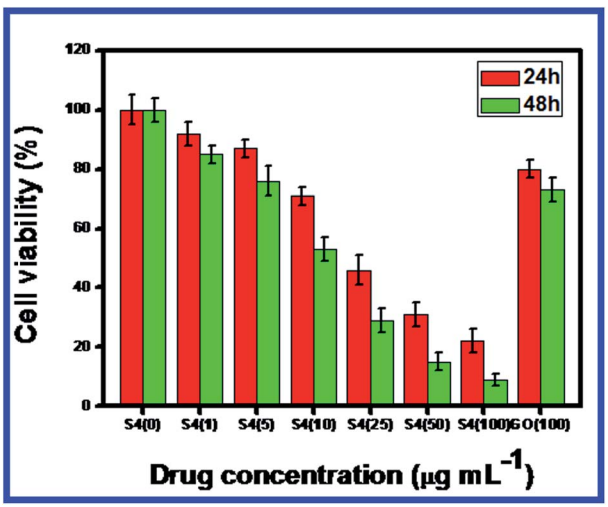

Fig. 4 Cell viability of human tumorous OCM-1 cells incubated with different amounts of SBG prepared from $n_{starch} : n_{borate} : n_{GO}$ = 2 : 1 : 1 (S4) compared to 100 μg mL^{-1} GO after 24 h and 48 h.

antitumor drug can be developed based on the findings of the sample S4 (*i.e.* $n_{starch} : n_{borate} : n_{GO} = 2 : 1 : 1$).

For better understanding the antitumor performance of the sample S4, we further performed dose-dependent antitumor study with OCM-1 cells using the sample S4. Concentrations of S4 were varied from 1 to 100 μg mL^{-1}. Fig. 4 shows the OCM-1 cell viability incubated with different amounts of S4 after 24 h and 48 h. It is found that the antitumor ability of S4 exhibits a significant dose-dependent trend. More than 70% tumor cells exhibited a strong suppression rate after 48 h incubation when over 25 μg mL^{-1} SBG (at the ratio according to S4) was introduced, confirming the outstanding antitumor ability of the resulting SBG.

Conclusions

In summary, we have designed and successfully synthesized a series of high-performance novel antitumor drugs from starch–borate–GO nanocomposites using a simple but efficient method. Successful synthesis of SBG nanocomposite was confirmed by various spectroscopic techniques including FTIR, TEM, Raman, and XPS. The GO with rich oxygen-containing functional groups demonstrated strong interactions with starch complex *via* a borate linker. Good dispersibility of the as-synthesized SBG in aqueous solution and cell culture media indicated that the inclusion of starch enhanced the dispersibility of the nanocomposites. The SBG nanocomposite (prepared from $n_{starch} : n_{borate} : n_{GO} = 2 : 1 : 1$) showed excellent biocompatibility with ARPE-19 cells (more than 90% cell viability) while exhibited superb antitumor ability against the OCM-1 cells (with less than 20% cell survival rate). The antitumor ability of SBG was further found to be dose-dependent, suggesting that the as-prepared SBG nanocomposite discovered in the present work is a novel highly-efficient targeted antitumor drug which may provide new insights into the development of a new class of inorganic-polymer drugs.

Acknowledgements

Financial supports for this work from the Chinese National Nature Science Foundation (21405115, 21374081, 51433005), Wenzhou Bureau of Science and Technology (Y20120218), Zhejiang Provincial Medical and Health Project (2015KYB254) and Eye Hospital of Wenzhou Medical University (YNCX201408) are acknowledged.

References

1 G. Nicola, S. Peddi, M. Stefanova, R. A. Nicholas, W. G. Gutheil and C. Davies, *Biochemistry*, 2005, **44**, 8207.
2 T. R. Transue, J. M. Krahn, S. A. Gabel, E. F. DeRose and R. E. London, *Biochemistry*, 2004, **43**, 2829.
3 F. H. Nielsen, *Nutr. Today*, 1992, **27**, 6.
4 L. Dinca and R. Scorei, *J. Nutr. Ther.*, 2013, **2**, 22.
5 S. A. Hubbard, *Biol. Trace Elem. Res.*, 1998, **66**, 343.
6 F. S. Kot, *Rev. Environ. Sci. Biotechnol.*, 2009, **8**, 3.
7 Y. P. Fang, R. Takahashi and K. A. Nishinari, *Biomacromolecules*, 2004, **5**, 126.
8 U. Manna and S. Patil, *ACS Appl. Mater. Interfaces*, 2010, **2**, 1521.
9 K. Saita, S. Nagaoka, T. Shirosaki, M. Horikawa, S. Matsuda and H. Ihara, *Carbohydr. Res.*, 2012, **349**, 52.
10 S. Baker, C. Ding, T. Akama, Y. Zhang, V. Hernandez and Y. Xia, *Future Med. Chem.*, 2009, **1**, 1275.
11 V. M. Moreira, J. A. R. Salvador, S. Simões, F. Destro and R. Gavioli, *Eur. J. Med. Chem.*, 2013, **63**, 46.
12 H. Yang, K. R. Landis-Piwowar, D. Chen, V. Milacic and Q. P. Dou, *Curr. Protein Pept. Sci.*, 2008, **9**, 227–239.
13 R. C. Kane, A. T. Farrel, R. Sridhara and R. Pazdur, *Clin. Cancer Res.*, 2006, **12**, 2955.
14 J. Su, F. Chen, V. Cryns and P. B. Messersmith, *J. Am. Chem. Soc.*, 2011, **133**, 11850.
15 G. Crini and P. M. Badot, *Int. J. Environ. Technol. Manage.*, 2010, **12**, 129.
16 C. N. R. Rao, A. K. Sood, K. S. Subrahmanyam and A. Govindaraj, *Angew. Chem., Int. Ed.*, 2009, **48**, 7752.
17 A. K. Geim and K. S. Novoselov, *Nat. Mater.*, 2007, **6**, 183.
18 K. T. Nguyena and Y. Zhao, *Nanoscale*, 2014, **6**, 6245.
19 M. Lin, R. Zou, H. Shi, S. Yu, X. Li, R. Guo, L. Yan, G. Li, Y. Liu and L. Dai, *Mater. Sci. Eng., C*, 2015, **50**, 300.
20 S. Agarwal, X. Zhou, F. Ye, Q. He, G. C. K. Chen, J. Soo, F. Boey, H. Zhang and P. Chen, *Langmuir*, 2010, **26**, 2244.
21 X. Yang, X. Zhang, Z. Liu, Y. Ma, Y. Huang and Y. Chen, *J. Phys. Chem. C*, 2008, **112**, 17554.
22 Z. Liu, J. T. Robinson, X. Sun and H. Dai, *J. Am. Chem. Soc.*, 2008, **130**, 10876.
23 K. Yang, S. Zhang, G. Zhang, X. Sun, S. T. Lee and Z. Liu, *Nano Lett.*, 2010, **10**, 3318.
24 R. M. Cheng, R. T. Zou, S. J. Ou, R. Guo, R. Y. Yan, H. Y. Shi, S. S. Yu, X. J. Li, Y. X. Bu, M. M. Lin, Y. Liu and L. M. Dai, *Polym. Chem.*, 2015, **6**, 2401.
25 W. Zhang, X. Li, R. Zou, H. Wu, H. Shi, S. Yu and Y. Liu, *Sci. Rep.*, 2015, **5**, 11129.
26 D. Li, M. B. Muller, S. Gilje, R. B. Kaner and G. G. Wallace, *Nat. Nanotechnol.*, 2008, **3**, 101.
27 M. Labet, W. Thielemans and A. Dufresne, *Biomacromolecules*, 2007, **8**, 2916.
28 Y. Guo, S. Guo, J. Ren, Y. Zhai, S. Dong and E. Wang, *ACS Nano*, 2010, **4**, 4001.
29 X. G. Sun, C. Liao, L. Baggetto, B. Guo, R. R. Unocic, G. M. Veith and S. Dai, *J. Mater. Chem. A*, 2014, **2**, 7606.
30 Z. Chen, D. Yu, W. Xiong, P. Liu, Y. Liu and L. Dai, *Langmuir*, 2014, **30**, 3567.
31 V. Chandra, J. Park, Y. Chun, J. W. Lee, I. C. Hwang and K. S. Kim, *ACS Nano*, 2010, **4**, 3979.
32 D. A. Kron, B. T. Hollan, R. Wipson, C. Mareke and A. Stein, *Langmuir*, 1999, **15**, 8300.
33 B. Sreedhar, M. Sairam, D. K. Chattopadhyay, P. A. S. Rathnam and D. V. M. Rao, *J. Appl. Polym. Sci.*, 2005, **96**, 1313.
34 L. Yan, M. Lin, C. Zeng, Z. Chen, X. Zhao, A. Wu, Y. Wang, S. Zhang, J. Qu, L. Dai, M. Guo and Y. Liu, *J. Mater. Chem.*, 2012, **22**, 8367.
35 L. Yan, Y. Wang, X. Xu, C. Zeng, J. Hou, M. Lin, J. Xu, F. Sun, X. Huang, L. Dai, F. Lu and Y. Liu, *Chem. Res. Toxicol.*, 2012, **25**, 1265.

